# Response and transit times in quantum-well structures

E. Runge and H. Ehrenreich
*Division of Applied Sciences, Harvard University, Cambridge, Massachusetts 02138*
(Received 7 January 1992)

The response of a biased double-barrier quantum well to a small ac voltage with characteristic time $\tau_{\rm resp}$ and the transit or dwell time $\tau_{\rm trans}$ are calculated using nonequilibrium Green's-function techniques. The tunneling process is shown to be predominantly sequential for an $In_xGa_{1-x}As/In_yAl_{1-y}As$ structure due to only well alloy scattering treated in the coherent-potential approximation. The magnitudes of $\tau_{\rm resp}$ and $\tau_{\rm trans}$ are in close agreement and about the same for either sequential or coherent tunneling.

This paper introduces a technically significant time for tunneling in a double-barrier quantum well (DBQW), viewed as a response time $\tau_{\rm resp}$ to a weak oscillatory field applied to a biased structure along any point of its current-voltage (*I-V*) characteristic. Its magnitude is calculated using nonequilibrium Green's-function techniques. It is shown to be nearly the same as the transit time $\tau_{\rm trans}$ defined and measured by Chemla and coworkers.[1,2] Furthermore, the paper demonstrates that sequential tunneling strongly dominates resonant tunneling[3,4] as a result only of weak III-V alloy scattering, for example, in the well of a lattice-matched $In_xGa_{1-x}As/In_yAl_{1-y}As$ structure described within the coherent-potential approximation (CPA).[5,6] The magnitude of $\tau_{\rm resp}$ or $\tau_{\rm trans}$, however, is only weakly dependent on the details of the tunneling process.

Aside from their intrinsic physical interest, these results are important since negative-differential-resistance diodes or DBQW are prototypical circuit components in cellular automata in which each cell is required to have high-frequency response and to be "locally interacting," i.e., decoupled from all but its nearest neighbors. Decoupling can be achieved if wave-function coherence between adjacent cells is eliminated. The dominance of sequential tunneling processes, which eliminate coherence, is therefore important.

Specifically, $\tau_{\rm resp}^{-1}$ is defined as the frequency, $\omega_{\rm resp}$, for which the imaginary part of the conductivity $\sigma(\omega)$ is maximum. This response time, which is appropriate for high-frequency applications, is physically different from the transit time $\tau_{\rm trans}$ defined as the ratio of the charge density in the well to the current density, $\rho_W/j_{\rm dc}$, at arbitrary bias.

The model of a biased symmetric DBQW to be used in this analysis is shown in Fig. 1. The well having width $d_W$ is surrounded by two barriers having height $\Lambda_S$ and width $d_S$ where $S=L$ (left) or $R$ (right). The Fermi levels $\mu_L$ and $\mu_R$ in the leads represent the effect of charge accumulation in $L$ and depletion in $R$. The semiconductor alloys ($In_xGa_{1-x}As$ ) in the $L,R$ and well ($W$) regions are assumed to be the same, as are those of the barriers ($In_yAl_{1-y}As$). The potential drop across the structure is modeled by a stepwise constant potential energy having values $\Phi_L=eV_{\rm dc}$, where $V_{\rm dc}$ is the voltage drop, $\Phi_W=\frac{1}{2}\Phi_L$ for a symmetric DBQW, and $\Phi_R=0$. The tunneling matrix element through the barrier, $h_{SW}$, is given within the WKB approximation. The well is assumed to contain only one resonant level $E_0$ in the absence of alloying effects. $E_0$ represents the edge of a two-dimensional conduction band (CB) with energy $\Phi_W+E_0+\varepsilon_{k_\parallel}$, where $k_\parallel$ are associated with the two-dimensional continuum perpendicular to the growth axis and $\varepsilon_{k_\parallel}=\hbar^2k_\parallel^2/2m^*$.

The Hamiltonian is given as a sum of terms $H_S^0$ unperturbed by barrier tunneling and well scattering and others, $H_{SW}^{\rm tun}$ and $H_W^{\rm scat}$, describing the remaining effects. Explicitly, in terms of appropriately labeled creation and annihilation operators,

$$H_S^0=\begin{cases}\sum_{\mathbf{k}}(\varepsilon_{\mathbf{k}}+\Phi_S)c_{S\mathbf{k}}^\dagger c_{S\mathbf{k}}\ , & S=L,R\\ \sum_{k_\parallel}(E_0+\varepsilon_{k_\parallel}+\Phi_W)c_{Wk_\parallel}^\dagger c_{Wk_\parallel}\ , & S=W\ ,\end{cases}\tag{1}$$

where $\mathbf{k}=(k_\parallel,k_z)$ refers to the $L$ and $R$ regions and

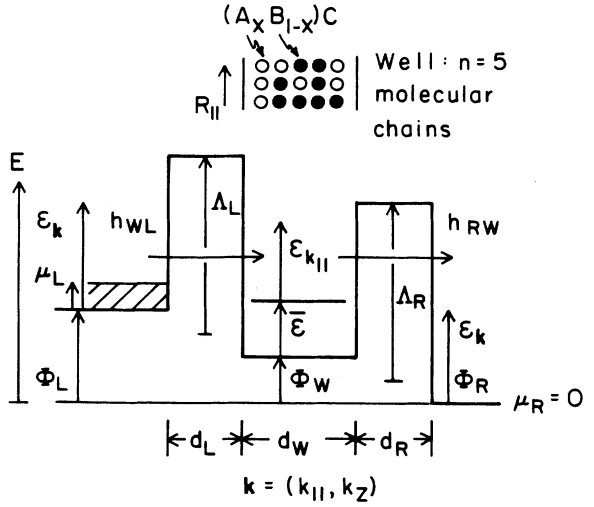


FIG. 1. Model of biased DBQW structure. Barrier and well dimensions defined in text; alloy well resonance level $\bar{\varepsilon}$; Fermi level $\mu_L,\mu_R$; tunneling amplitudes $h_{WL},h_{RW}$. Inset: Arrangement of random molecular chains having $n=5$ *AC* (open) or *BC* (closed) molecules for $(A_xB_{1-x})C$ well alloy.

 

$\varepsilon_{\mathbf{k}}=\hbar^2\mathbf{k}^2/2m^*$. Further

$$H_{WS}^{\text{tun}}=\sum_{k_z,k_\parallel}(h_{WS}c_{Wk_\parallel}^{\dagger}c_{S\mathbf{k}}+\text{H.c.}) \tag{2}$$

and

$$H_W^{\text{scat}}=\sum_{R_\parallel}(\varepsilon_{R_\parallel}-E_0)c_{WR_\parallel}^{\dagger}c_{WR_\parallel} \tag{3}$$

in a representation using two-dimensional Wannier creation operators $c_{WR_\parallel}^{\dagger}$. As indicated in the inset of Fig. 1, a row of atoms along the growth direction is visualized as an $n$-membered molecular chain consisting of randomly disordered $AC$ and $BC$ molecules constituting the $(A_xB_{1-x})C$ alloy. The position of each chain is defined by a value of $\mathbf{R}_\parallel$ as indicated in Fig. 1. The resulting two-dimensional alloy scattering associated with each of the randomly distributed chains is the only scattering effect to be considered here. Even though scattering is weak for III-V alloys, it causes tunneling to be largely sequential. The scattering potential due to the configuration-dependent energy

$$\varepsilon_{R_\parallel}=\bar{\varepsilon}+\sum_i|\phi(z_i)|^2(\varepsilon_i-\bar{\varepsilon}) \tag{4}$$

for each chain, where $i=1,2,\ldots,n$ labels the sequence of $AC$ and $BC$ molecules with on-site electronic energies $\varepsilon_A,\varepsilon_B$, respectively, is much weaker than the confinement kinetic energy $E_0$. Here $\bar{\varepsilon}=x\varepsilon_A+(1-x)\varepsilon_B$ denotes the virtual crystal CB edge; $\bar{\varepsilon}$ replaces $E_0$ in the alloy case; $\varepsilon_A-\varepsilon_B$ is the CB offset between the $AC$ and $BC$ crystals.

Equation (4) gives the chain energies to first order in the scattering. $\phi(z_i)$ is the normalized envelope function along the growth axis. The $\varepsilon_{R_\parallel}$ are assumed to have a Gaussian distribution with probability $(\Delta\sqrt{2\pi})^{-1}\exp[-(\varepsilon_{R_\parallel}-\bar{\varepsilon})^2/2\Delta^2]$ and a variance

$$\Delta^2=x(1-x)(\varepsilon_A-\varepsilon_B)^2\left[(d_W/n)\int_W dz|\phi(z)|^4\right],$$

where the integral extends over the well width $d_W$ and has the value $3/(2d_W)$ for deep wells. The CPA description of Gaussian disorder has been considered previously.[7]

A nonequilibrium Green's-function formalism must be used to calculate the current since inelastic-scattering processes are neglected here, and are insufficient to achieve equilibrium in the well region at low $T$ in any case. The advanced and retarded Green's functions $G^a$, $G^r$, and also $G^<$ are related by Dyson's equations.[8,9] The quantities of particular physical interest obtained from a solution of these equations are the matrix elements of the configuration averaged well Green's functions

$$G^r(Wk_\parallel,Wk'_\parallel;E)=\delta_{k_\parallel k'_\parallel}[E-(\bar{\varepsilon}+\varepsilon_{k_\parallel}+\Phi_W)-\Sigma_L(k_\parallel;E)-\Sigma_R(k_\parallel;E)-\Sigma_{\text{CPA}}(E)]^{-1} \tag{5}$$

and

$$G^<(Wk_\parallel,Wk_\parallel;E)=-\phi_W(E)[G^r(Wk_\parallel,Wk_\parallel;E)-G^a(Wk_\parallel,Wk_\parallel;E)]=2\pi i\phi_W(E)A(k_\parallel,E). \tag{6}$$

In Eq. (5), $\Sigma_L$ and $\Sigma_R$ are the self-energies associated with tunneling processes out of the well $W$ to $L$ and $R$, respectively, and $\Sigma_{\text{CPA}}$ is associated with disorder scattering in the well. We shall assume the self-energy shift to be absorbed in $\bar{\varepsilon}$. The remaining part,

$$i\,\text{Im}[\Sigma_{S=L,R}]=-i\pi|h_{WS}|^2\sum_{k_z}\delta(E-\varepsilon_{\mathbf{k}}-\Phi_S)\equiv-\tfrac{1}{2}i\Gamma_S \tag{7}$$

and $i\,\text{Im}[\Sigma_{\text{CPA}}]=-\frac{1}{2}i\Gamma_{\text{scat}}$ describes the broadening due to tunneling and scattering, respectively. $\Gamma_S$ is the resonant level width associated with the escape time through the barrier at side $S=L,R$. $\Gamma_{\text{CPA}}$ (not defined explicitly here) is the energy-dependent level width associated with scattering. It is obtained from a numerical solution of the CPA equations. The tunneling process through the DBQW is seen to be largely coherent if $\Gamma_{\text{CPA}}\ll\Gamma_L,\Gamma_R$ and sequential in the opposite limit.

Equation (6) contains $\phi_W(E)$, the nonequilibrium distribution of electrons in the well. This form[9] is analogous to $G_0^<(S\mathbf{k},S\mathbf{k};E)$, the unperturbed function in the $L$ and $R$ regions, in which $\phi_W(E)$ is replaced by the equilibrium Fermi distributions $f_L(E-\Phi_L)$ and $f_R(E)$.[10] $A(k_\parallel,E)$ is the spectral density associated with the state $k_\parallel$.

The dc current density (per unit area) $j_{\text{dc}}$ is obtained by calculating the $S\rightarrow W$ current density $j_{S\rightarrow W}=2e(\partial/\partial t)\hat{N}_S$ where $\hat{N}_S=\sum_{\mathbf{k}}c_{\mathbf{k}S}^{\dagger}c_{\mathbf{k}S}$ and expressing the result in terms of the Green's functions. The well distribution is obtained from current conservation $j_{L\rightarrow W}=j_{W\rightarrow R}$:

$$\phi_W(E)=[\Gamma_Lf_L(E-\Phi_L)+\Gamma_Rf_R(E)]/(\Gamma_L+\Gamma_R). \tag{8}$$

The remarkably simple formal result is

$$j_{\text{dc}}=\frac{2e}{\hbar}\int_{-\infty}^{\infty}dE\frac{\Gamma_L\Gamma_R}{\Gamma_L+\Gamma_R}g_W(E)[f_L(E-\Phi_L)-f_R(E)], \tag{9}$$

where $g_W(E)=\int A(k_\parallel,E)d^2k_\parallel/(2\pi)^2$ is the two-dimensional well density of states. We note that the *form* of Eqs. (8) and (9) is that expected when the tunneling is purely sequential. The same formal result is obtained by considering the purely coherent tunneling limit obtained by setting $\Sigma_{\text{CPA}}=0$. The bias dependence of this nonlinear $I$-$V$ dependence is indicated explicitly. Except for its dependence on $V_{\text{dc}}$, the $\Gamma_S$ may be assumed constant since the resonance width is $<1$ meV, except when $V_{\text{dc}}$ is such that the well CB edge coincides energetically with that of the CB on the left (in the negative-resistance region).

The level broadening associated with tunneling and scattering is contained entirely in $g_W(E)$. The spectral densities with and without scattering, $A(k_\parallel=0,E)$, are compared in Fig. 2 for the state at the well CB edge when

it lies just above (0.2 meV) the left CB edge in the absence of scattering for a lattice matched $In_{0.53}Ga_{0.47}As/In_{0.52}Al_{0.48}As$ DBQW with $d_W=45$ A and $d_L=d_R=56$ A. This illustrative example corresponds to sample $A$ of Ref. 1 which was measured at 10 K. We set $\mu_L=50$ meV. Scattering effects shift the CB edge by $\mathrm{Re}[\Sigma_{CPA}]$ as indicated. To permit comparison, the Lorentzian resonant peak associated with tunneling has been shifted by $\mathrm{Re}[\Sigma_{CPA}]$. The shape of $A(0,E)$ including scattering is strongly asymmetric. This behavior results from the Gaussian distribution of states that blur the CB edge: The high-energy tail results from the increasing density of state available for scattering; the sharp cutoff at low energies is primarily associated with the energy dependence of $\mathrm{Re}[\Sigma_{CPA}]$. Both widths are small compared to $eV_{dc}$. Since the $f_S$ and $\Gamma_S$ in Eq. (9) are weakly dependent on energy when $eV_{dc}$ lies well within the Ohmic (positive-differential-resistance) region, the energy integral reduces to $\int dE\, g_W(E+\Phi_W)$ and is the same for all reasonable alloy scattering strengths. *As a result* $j_{dc}$ in these regions is unaffected by scattering,[11] and *will be the same regardless of whether the transport is coherent or sequential.* Thus, neither $\tau_{resp}$ nor $\tau_{trans}$ will be appreciably affected by the tunneling mechanisms. Note also that *I-V* measurements cannot be used to distinguish between coherent and sequential tunneling.

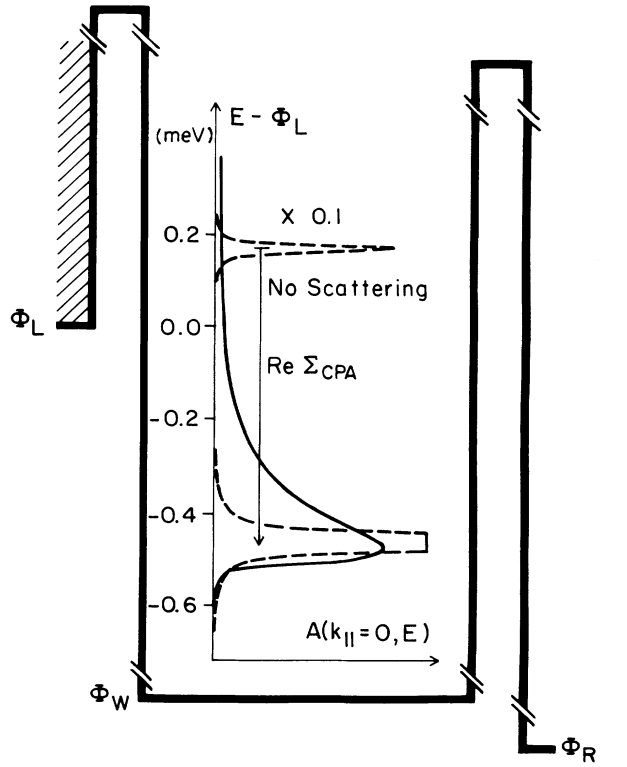


FIG. 2. Spectral density $A(k=0,E)$ for biased DBQW at far end of negative-differential-resistance regime with (solid curve) and without (dashed curve) alloy scattering. Resonance is sharper and located in positive-differential-resistance region for the case of well lifetime broadening alone (upper dashed curve; multiplied by 0.1). Shift by $\mathrm{Re}[\Sigma_{CPA}]$ and scale change permits comparison between line shapes. DBQW is indicated schematically. Dashed region on left occupied by electrons.

For a given $V_{dc}$, the factor $\Gamma_L\Gamma_R/(\Gamma_L+\Gamma_R)$ may be removed from the integral in Eq. (9). Similarly, the contribution to the current from unscattered electrons can be shown to be $j_{dc}\propto\Gamma_L\Gamma_R/(\Gamma_L+\Gamma_R+\Gamma_{scat})$. The fraction of coherent tunneling is thus $(\Gamma_L+\Gamma_R)/(\Gamma_L+\Gamma_R+\Gamma_{scat})$. Its value is about 1% for sample $A$ of Ref. 1.

The transit time, $\tau_{trans}=\rho_W/j_{dc}$, where

$$\rho_W=\int_{-\infty}^{\infty} dE\,\phi_W(E)g_W(E) \tag{10}$$

is the charge density in the well, was measured by Chemla and co-workers[1] using differential absorption spectroscopy. Figure 3 compares the measured and calculated $\tau_{trans}$ in the Ohmic region as a function of current density for sample $A$ of Ref. 1. The range of current densities for the experimental points is larger than that for the calculations because the experimental maximum current density exceeds the calculated value. The factor of 3–4 difference is reasonable in view of the approximations inherent in the model, the neglect of other scattering effects,[12] and the exponential dependence of $h_{WS}$ on input parameters.

$\tau_{trans}$ may be estimated simply when $\bar{\varepsilon}$ is aligned with filled states on the left and empty states on the right. Equations (8)–(10) yield $\tau_{trans}\sim\hbar/\Gamma_R\approx 75$ ps in the present case when $j_{dc}=100$ A/cm$^2$, in agreement with the physical expectation that the transit time is controlled by the effective height of the right barrier.

The importance of the frequency response of a DBQW operating as a negative-differential-resistance diode characterized by the response time $\tau_{resp}$ has already been noted. Operationally, the appropriately biased DBQW,

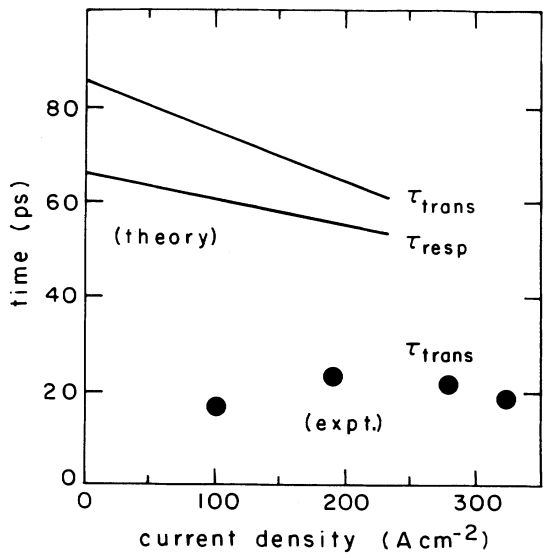


FIG. 3. Theoretical response and transit times vs current density compared with experiment, sample $A$, Ref. 1, in positive-differential-resistance region.

acted upon by an additional small ac field having frequency $\omega$ with Hamiltonian

$$H_{\rm ac}=\tfrac{1}{2}eV_{\rm ac}(\hat{N}_L-\hat{N}_R)e^{-i\omega t}$$

responds linearly to that field. For frequencies $\omega>\omega_{\rm resp}$, as defined above, the current is no longer able to follow $H_{\rm ac}$ without phase lag. The upper frequency limit of device operation is thus given by $\omega_{\rm resp}=\tau_{\rm resp}^{-1}$. (The frequency limit is depressed due to circuit capacitance effects and other scattering mechanisms.)

The derivation of $\sigma(\omega)$ is lengthy, since a Bethe-Salpeter equation must be solved to include vertex corrections properly.[13] The result, valid for the Ohmic region in which the energy dependence of the $\Gamma_S$ can be neglected, is

$$\sigma(\omega)=\frac{e^2}{2\hbar^2\omega}\int_{-\infty}^{\infty}dE\,g_W(E;\omega)\frac{(\hbar\omega+2i\Gamma_R)\Gamma_L(\Delta f_L)+(\hbar\omega+2i\Gamma_L)\Gamma_R(\Delta f_R)}{\hbar\omega+i(\Gamma_L+\Gamma_R)}\ , \tag{11}$$

where

$$g_W(E;\omega)=(-2\pi i)^{-1}[F^r_{\rm CPA}(E+\hbar\omega)-F^a_{\rm CPA}(E)]\ ,$$

$$F^{r(a)}_{\rm CPA}=\langle 0|G^{r(a)}_{\rm CPA}(E)|0\rangle\ ,$$

the single-chain diagonal matrix element of the CPA retarded (advanced) Green's function, and $\Delta f_S=f_S(E+\hbar\omega-\Phi_S)-f_S(E-\Phi_S)$ $(S=L,R)$. Note that $g_W(E;0)=g_W(E)$, the well density of states in Eq. (9), and that $\sigma(0)=dj_{\rm dc}/dV_{\rm dc}$ at a given $V_{\rm dc}$ in the present case. The applied dc voltage remains even when $V_{\rm ac}$, which is much smaller than $V_{\rm dc}$, has vanishing frequency.

The results for $\tau_{\rm resp}$ are also shown in Fig. 3. Even though the physical ingredients in the definitions of $\tau_{\rm trans}$ and $\tau_{\rm resp}$ are quite different, the numerical values are seen to be in remarkably close agreement. Calculations for a typical current of $j_{\rm dc}=100$ A/cm$^2$ in the *negative*-differential-resistance region (not indicated in Fig. 3) show that $\tau_{\rm trans}$ and $\tau_{\rm resp}$ have values about 60 ps and differ by only 7 ps, as in the Ohmic region. This result confirms that the experimentally accessible time defined and measured in Ref. 1 is, in fact, useful in device applications of current interest.

We are grateful to D. S. Chemla, D. K. Ferry, and P. M. Hui for useful discussions. This work was supported by the U.S. Joint Services Electronics Program (JSEP) through ONR Contract No. N00014-89-J-1023 and by the DARPA through ONR Contract No. N00014-86-K-0033.

[1] I. Bar-Joseph, T. K. Woodward, D. S. Chemla, D. Sivco, and A. Y. Cho, Phys. Rev. B **41**, 3264 (1990).

[2] I. Bar-Joseph *et al.*, Superlatt. Microstruct. **8**, 409 (1990).

[3] S. Luryi, in *Heterojunction Band Discontinuities: Physics and Device Applications*, edited by F. Capasso and G. Margaritondo (Elsevier, Amsterdam, 1987), p. 489.

[4] B. Ricco and M. Ya. Azbel, Phys. Rev. B **29**, 1970 (1984).

[5] For example, H. Ehrenreich and L. M. Schwartz, in *Solid State Physics*, edited by H. Ehrenreich, F. Seitz, and D. Turnbull (Academic, New York, 1976), Vol. 31, p. 149.

[6] B. Velický, Phys Rev. **184**, 614 (1969).

[7] H. Sumi and Y. Toyozawa, J. Phys. Soc. Jpn. **31**, 342 (1971).

[8] For example, J. Rammer and H. Smith, Rev. Mod. Phys. **58**, 323 (1986).

[9] L. Y. Chen and C. S. Ting, Phys. Rev. Lett. **64**, 3159 (1990); Phys. Rev. B **41**, 8533 (1990); **43**, 2097 (1991).

[10] Note that in the $S$ regions both $G^r$ and $G^a$ also assume their unperturbed values.

[11] This fact was previously noted for a simple resonance model by T. Weil and B. Vinter, Appl. Phys. Lett. **50**, 1281 (1987); M. Jonson and A. Grincwajg, *ibid.* **51**, 1729 (1987).

[12] For example, F. Chevoir and B. Vinter, Appl. Phys. Lett. **55**, 1859 (1989); H. A. Fertig, S. He, and S. Das Sarma, Phys. Rev. B **41**, 3596 (1990); J. Leo and A. H. MacDonald, *ibid.* **43**, 9763 (1991); N. S. Wingreen, K. W. Jacobsen, and J. W. Wilkins, *ibid.* **40**, 11 834 (1989).

[13] E. Runge and H. Ehrenreich (unpublished).